Noise Analysis of Ion Channels in Non-Space-Clamped Cables: Estimates of Channel Parameters in Olfactory Cilia

H. P. Larsson,* S. J. Kleene,# and H. Lecar*
*Department of Molecular and Cell Biology, University of California Berkeley, Berkeley, California 94720, and #Department of Cell Biology, Neurobiology and Anatomy, University of Cincinnati, Cincinnati, Ohio 45267-0521, USA

ABSTRACT Ion channels in the cilia of olfactory neurons are part of the transduction machinery of olfaction. Odorant stimuli have been shown to induce a biphasic current response, consisting of a cAMP-activated current and a Ca^{2+}-activated Cl^- current. We have developed a noise analysis method to study ion channels in leaky cables, such as the olfactory cilium, under non-space-clamp conditions. We performed steady-state noise analysis on ligand-induced currents in excised cilia, voltage-clamped at input and internally perfused with cAMP or Ca^{2+}. The cAMP-activated channels analyzed by this method gave results similar to those of single-channel recordings (γ = 8.3 pS). Single-channel currents have not yet been recorded for the Ca^{2+}-activated Cl^- channels. Using our noise analysis method, we estimate a unit conductance, γ = 0.8 pS, for these channels. The density of channels was found to be ~70 channels/μm^2 for both channel species.

INTRODUCTION

In vertebrates, odorous stimuli are transduced into receptor currents in the cilia of olfactory receptor neurons (Kurahashi, 1989; Firestein et al., 1990; Lowe and Gold, 1991). One second messenger for olfactory transduction is cyclic AMP (reviewed in Zufall et al., 1994; Restrepo et al., 1996). Cyclic AMP directly gates channels in the ciliary membrane (Nakamura and Gold, 1987), allowing a depolarizing influx of cations, including Ca^{2+} (Kurahashi and Shibuya, 1990; Frings et al., 1995). Ca^{2+} in the cilium can then activate a secondary receptor current carried by Cl^- (Kleene and Gesteland, 1991b; Kurahashi and Yau, 1993; Kleene, 1993; Lowe and Gold, 1993).

Two advantages have been proposed for this sequence of receptor currents. First, in aquatic vertebrates whose olfactory endings are bathed in fresh water, a Cl^- efflux might be the only way to generate a depolarizing receptor current (Kurahashi and Yau, 1993, 1994; Kleene and Pun, 1996). Second, the Ca^{2+}-activated Cl^- current can greatly amplify the primary cationic current (Kleene, 1993; Lowe and Gold, 1993; Zhainazarov and Ache, 1995; Kleene, 1996). In intact receptor neurons, up to 85% of the receptor current induced by odorous stimulation may be carried by Cl^- (Lowe and Gold, 1993).

The fidelity of amplification by the Cl^- current should depend in part on the unit conductance of the underlying single channels. Preliminary evidence suggested that the unit conductance was very small. In general, one can infer the unit conductance of even a small channel through fluctuation analysis of the macroscopic current (Lecar and Sachs, 1981; DeFelice, 1981). Under effective space clamp, the variance introduced by ion channels will be proportional to the square of the unit conductance (Lecar and Sachs, 1981; DeFelice, 1981).

However, determining the unit conductance of the Cl^- channels was not straightforward. When a large current is activated in a cilium, the cilium cannot be voltage-clamped along its entire length. This is due to the cable-conduction properties of the long, thin cilium (Kleene et al., 1994). More current will be detected from a channel near the tip of the recording pipette than from a distant channel. We provide a theoretical model that allows fluctuation analysis of voltage-independent channels in a cable such as the olfactory cilium. The analysis suggests that the unit conductance of the ciliary Cl^- channel is just 0.8 pS.

MATERIALS AND METHODS

Ciliary patch method

Single receptor neurons were isolated from olfactory epithelium of the northern grass frog *Rana pipiens* as described elsewhere (Kleene and Gesteland, 1991a). Cell suspensions were prepared in the standard extracellular solution (Table 1). A single receptor neuron was placed in an extracellular bath. One cilium of a neuron was sucked into a patch pipette until a high-resistance seal formed near the base of the cilium. The pipette was raised briefly into the air, causing excision of the cilium from the cell. The cilium remained sealed inside the recording micropipettete with the cytoplasmic face of the membrane exposed to the bath. The pipette containing the cilium could be quickly transferred through the air to various pseudointracellular baths without rupturing the seal. The patch procedure was videotaped, and ciliary lengths were estimated by playing back the video images one frame at a time. The external axial resistance between the conical recording pipette (pipette tip diameter = 0.5 μm) and the cilium is estimated to be a magnitude smaller than the internal axial resistance of the cilium (diameter = 0.28 μm). The external axial resistance has therefore been omitted in the calculation of axial resistance (see Theory). Additional details of the ciliary patch procedure have been presented elsewhere (Kleene and Gesteland, 1991a; Kleene, 1995).

Received for publication 26 August 1996 and in final form 26 November 1996.

Address reprint requests to Dr. Harold Lecar, Department of Molecular and Cell Biology, University of California–Berkeley, 229 Stanley Hall, Berkeley, CA 94720. Tel.: 510-643-8875; Fax: 510-643-9290; E-mail: hlecar@uclink4.berkeley.edu.

0006-3495/97/03/1193/11 $2.00

TABLE 1 Compositions of solutions (mM)

	Extracellular					
	NaCl	KCl	$CaCl_2$	$MgCl_2$	EDTA	NaOH
Standard	115	3	1	2	—	1
cAMP study	115	—	—	—	1	4
Ca^{2+} study	117	1.14	1	2	—	1

	Pseudointracellular						
	NaCl	cAMP	$CaCl_2$	$MgCl_2$	BAPTA	Dibromo-BAPTA	NaOH
cAMP study	115	0.00005–0.1	1		2	—	9
Ca^{2+} study	115	—	0.12–2.29	2	—	2	1

BAPTA, 1,2-bis(2-aminophenoxy)ethane-*N,N,N′,N′*-tetraacetic acid; dibromo-BAPTA, 1,2-bis(2-amino-5-bromophenoxy)ethane-*N,N,N′,N′*-tetraacetic acid, tetrapotassium salt. All solutions contained 5 mM HEPES and were adjusted to pH 7.2. The NaOH listed includes amounts necessary to titrate EDTA and BAPTA, which are listed as free acids.

Solutions

The solutions used are listed in Table 1. To study noise due to the cAMP-gated cationic channel, divalent cations were removed from the external solution. Internal $[Ca^{2+}]_{free}$ was buffered at 0.15 μM. In such solutions, single cAMP-gated channels can be observed in small membrane patches (Zufall et al., 1991a, 1994; Frings et al., 1992; Kurahashi and Kaneko, 1993). Membrane noise was recorded with nine different concentrations of cAMP. Concentrations were chosen to give cAMP-activated conductances that ranged evenly between 5% and 100% of the maximum conductance, based on the dose-response curve.

Noise properties of the Ca^{2+}-activated Cl^- current were studied in solutions similar to those previously described (Kleene and Gesteland, 1991b). The half-maximum current is seen when cytoplasmic $[Ca^{2+}]_{free}$ is near 5 μM. Dibromo-1,2-bis(2-aminophenoxy)ethane-*N,N,N,N*-tetraacetic acid (dibromo-BAPTA) was used to effectively buffer $[Ca^{2+}]_{free}$ in this range. Previously reported constants and methods (Kleene and Gesteland, 1991b; Kleene and Cejtin, 1994) were used to calculate $[Ca^{2+}]_{free}$. Membrane noise was recorded with nine different values of $[Ca^{2+}]_{free}$. Concentrations were chosen to give Ca^{2+}-activated conductances that ranged evenly between 5% and 100% of the maximum conductance, based on the published dose-response relation (Kleene and Gesteland, 1991b).

For the cAMP study, K^+ was removed from solutions to reduce noise from the basal membrane conductance (Kleene, 1992) and to eliminate occasional large single channels. For the Ca^{2+} study, it was necessary to add dibromo-BAPTA as the tetrapotassium salt. In this case external K^+ was adjusted so that E_K was -50 mV, which was near the recording potential. This ensured that K^+ channels did not contribute to the measured noise. In all experiments, a current record was first taken with the cilium in a control bath (no cAMP or 0.1 μM free Ca^{2+}). The pipette containing the cilium was then moved through the nine baths with increasing concentrations of ligand. Finally, another record was taken in the control bath. On average, current increased by a factor of 1.21 ± 0.07 ($n = 13$) between the first and second control measurements, probably because of degradation of the seal over time.

Electrical recording

Both the recording pipette and chamber were coupled to a List L/M-EPC7 patch-clamp amplifier by Ag/AgCl electrodes. All recordings were made under voltage clamp at room temperature (25°C). The holding potential was -50 mV for the cAMP study and -40 mV for the Ca^{2+} study. Input conductance in the absence of second messenger was taken to be the slope of the current-voltage relation at the relevant holding potential. Current was adjusted to zero with the open pipette in the well in which the patching procedure was done. Corrections were made for liquid junction potentials at the pipette tip; these never exceeded 3 mV.

The amplifier signal was filtered at 3 kHz with an 8-pole low-pass Bessel filter (model 902L; Frequency Devices, Haverhill, MA). Frequency cutoffs of other elements in the system were all above 3 kHz. Current was sampled at 7 kHz by the Axotape program (Axon Instruments, Foster City, CA). Duration of the current records was 10 s for the variance-to-mean studies and 60 s for the power density spectra. Potentials are reported as bath (cytoplasmic) potential relative to pipette potential. Currents in this study were all inward currents but have been assigned positive values for convenience in plotting.

Theory: variance-to-mean relation for channel noise in a cable structure

We consider a finite cable (e.g., the olfactory cilium), which we voltage clamp at its input (the open end of a finite cable). The channel-induced current and current fluctuations measured at the input to the ciliary cable reflect the gating noise of channels in the cell membrane as well as the cable properties of the cilium. The tubular ciliary membrane containing ligand-gated channels behaves like a leaky cable, so that both the mean ligand-induced current and the current noise contributed by different segments of the cable decrease exponentially with distance from the cable input end. Because the variance power falls off more rapidly with distance than the mean current, the variance-to-mean ratio measured at input is in general smaller than the space-clamped value by a factor that depends on the cable length constant. The situation is further complicated because the cable length constant itself depends upon the membrane shunt conductance induced by open channels.

In a typical experiment, the channel-induced shunt conductance begins to dominate over the intrinsic leakiness at rather low open probability (depending on the conductance and density of the particular species of channel). To utilize the cable-noise data for estimating the unit conductance and density of the ciliary channels, we must fit the data to a nonlinear relation that incorporates the channel-induced changes to the cable properties. Thus we wish to derive the appropriate expressions for the variance and mean currents for this channel-loaded cable.

In this derivation, the cable parameters are approximated by their non-frequency-dependent (DC) values. This poses no problem because the channel noise is confined to frequencies lower than the low-pass frequency of the ciliary cable. The cable filtering depends on the cable time constant, which for a ciliary cable is on the order of 2×10^{-4} s ($\tau = R_m C_m$, where $R_m = 200\ \Omega\text{-cm}^2$ and $C_m = 10^{-6}$ F/cm^2). Thus, when we use the frequency dependence of the cable input impedance, the half-power point for the ciliary cable is approximately 1500 Hz, whereas the excess noise caused by channel gating is observed to fit a Lorentzian spectrum having a bandwidth of at most 700 Hz. The DC approximation can also be justified a posteriori by the observation of a Lorentzian spectrum rather than a cable-filtered spectrum for the agonist-induced noise.

For a finite cable with voltage at one end clamped to V_0, the voltage varies with distance x along the cable, as given by equation 4.10 by Jack et al. (1975):

$$V(x) = V_0 \frac{\cosh((x-d)/\lambda)}{\cosh(d/\lambda)}, \tag{1}$$

where d is the length of the cilium and λ is the space constant. λ depends on the axial resistance per unit length, r_i, and the membrane conductance per unit length, g_m, as

$$\lambda = (r_i g_m)^{-1/2}. \tag{2}$$

However, the membrane conductance is the sum of a basal leakage, g_0, and the conductance induced by ligand-gated channel openings (both per unit length),

$$g_m = g_0 + n\gamma p, \tag{3}$$

where γ is the unitary conductance, p is the probability of channel opening (which is independent of V), and n is the density of channels per unit cable length.

The space constant for the cable is now a variable function of open-channel probability and can be written as

$$\lambda(p) = [r_i g_0[1 + (n\gamma/g_0)p]]^{-1/2} = \lambda_0(1 + Kp)^{-1/2}, \tag{4}$$

where $\lambda_0 = (r_i g_0)^{-1/2}$ is the initial length constant before activation of the ligand-gated channels, and $K = n\gamma/g_0$ is a dimensionless parameter that characterizes the relative conductance induced by channels as compared to the basal cable conductance.

The mean current and variance can be calculated by summing the current components at input contributed by the fluctuating channels in each infinitesimal length of the cylindrical cable,

$$\bar{I} = (npi/V_0)\int_0^d V(x)\,dx, \tag{5a}$$

$$\mathrm{var}(I) = (np(1-p)i^2/V_0^2)\int_0^d [V(x)]^2\,dx, \tag{5b}$$

where i is the unitary channel current (for $V = V_0$). Substituting from Eq. 1, we can integrate explicitly,

$$\int_0^d V(x)\,dx = V_0\int_0^d \frac{\cosh((x-d)/\lambda)}{\cosh(d/\lambda)}\,dx = \lambda V_0 \tanh(d/\lambda). \tag{6}$$

Substituting Eq. 6 into Eq. 5a, the mean agonist-induced current is given in terms of cable length as

$$\bar{I} = npi\lambda(p)\tanh\left(\frac{d}{\lambda(p)}\right). \tag{7}$$

Similarly,

$$\int_0^d [V(x)]^2\,dx = V_0^2\,\mathrm{sech}^2(d/\lambda)[d/2 + (\lambda/4)\sinh(2d/\lambda)], \tag{8}$$

so that the the current variance for noise generated in the membrane is given by substituting Eq. 8 into Eq. 5b,

$$\mathrm{Var}(I) = np(1-p)i^2\lambda(p)\,\mathrm{sech}^2\left(\frac{d}{\lambda(p)}\right) \cdot \left[\frac{d}{2\lambda(p)} + 1/4\,\sinh\left(\frac{2d}{\lambda(p)}\right)\right]. \tag{9}$$

One way to infer i, the unitary channel current, and n, the linear density of channels, from the noise data is to plot the ratio r = variance/mean as a function of the mean current. In the ordinary space-clamped situation this would give the familiar linear plot,

$$r_{sc}(\bar{I}) = i(1-p) = i(1 - \bar{I}/(ndi)), \tag{10}$$

which intersects the vertical (r) axis at i and the horizontal ($\bar{I}$) axis at $\bar{I}_{max} = ndi$. For the cable, dividing Eq. 9 by Eq. 7, the ratio of variance-to-mean becomes

$$r(p) = i(1-p)\left[1/2 + \frac{d/\lambda(p)}{\sinh(2d/\lambda(p))}\right]. \tag{11}$$

The ratio, $r(p)$, plotted against mean current, $\bar{I}(p)$, can then be used to fit cable noise data. We note that for "short" cables, $d \ll \lambda$, and $r \to i(1-p)$, so that r versus $\bar{I}$ obeys the linear relation of Eq. 10. For $d \gg \lambda$–the limit of an infinite cable–the r vs $\bar{I}$ curve becomes a parabola,

$$r(\bar{I}) \approx i/2 - \bar{I}^2/(2g_0 n\lambda_0^2 V_0). \tag{12}$$

The intercept of this curve at $\bar{I} = 0$ gives exactly half the space-clamped value for the unitary current. For the infinite cable, the current intercept is given by

$$\bar{I}_{max} = (\lambda_0^2 g_0 V_0 ni)^{1/2}. \tag{13}$$

Thus the usual linear variance-to-mean ratio known for the space-clamped case is replaced by a set of more complex curves from which the single-channel current, i, and the channel density, n, can be extracted by fitting the data to the appropriate curve parameterized by $\lambda(p)$.

We wish to illustrate the extent of cable attenuation for different realistic situations. Experimentally, different cilia have different lengths and different basal space constants. Thus the cable correction for different cilia is best described in terms of a dimensionless parameter, $e(p) = d/\lambda(p)$.

From Eq. 4, we see how $e(p)$ varies with agonist dosage:

$$e(p) = e_0(1 + Kp)^{1/2}, \tag{14}$$

where $e_o = d/\lambda_o$ is a measure of the initial state of the cable. When the cable is short compared to the length constant, i.e., $e(p) < 1$, there is little attenuation along the cable, and the situation approximates the space-clamped limit. When $e(p) \gg 1$, we approach the limit of an infinite cable, for which only the channels within one length constant from the clamped end contribute to the observed channel noise. Thus as the agonist concentration is increased, more and more channels are open, but a smaller and smaller fraction of these channels actually contributes.

We use $e(p)$ for different cable lengths, shunt conductances, channel conductances, and densities to characterize the cable regime that applies. For the channel conductances and densities of interest in these experiments, we find that the results are insensitive to the value of e_o over the observed range of ciliary cable lengths. This is fortunate, because e_o is the experimental parameter that has the largest measurement uncertainty (because of the variability of the shunt resistance at the patch electrode seal). In the examples to follow, we use a value of $e_o = 0.4$, near the high end of our observed values, corresponding to a ciliary cable with $d = 30$ μm and $\lambda_0 = 75$ μm. For the basal membrane conductance per unit length, g_0, we used $g_0 = 5$ pS/μm, corresponding to the average of all the basal cable measurements.

In Fig. 1, we show $e(\bar{I})$ and $r(\bar{I})$ for hypothetical channels having two different values of unit conductance, $\gamma = 0.8$ pS (comparable to the

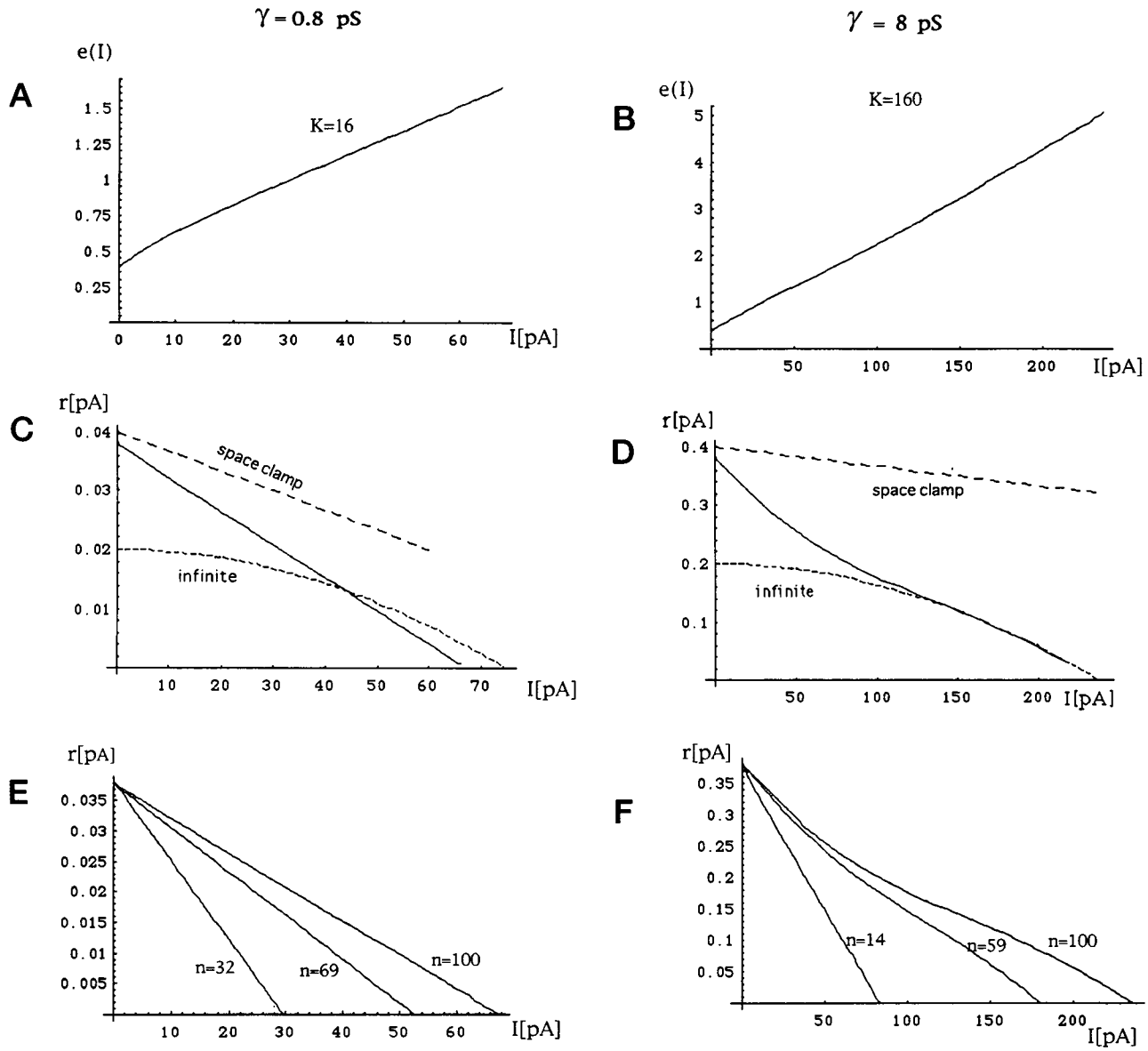

FIGURE 1 Theoretical corrections to variance/mean versus mean plots. Cable-correction parameters are calculated for 30-μm-long ciliary cables having low-conductance channels (γ = 0.8 pS) (*A*, *C*, *E*) and higher conductance channels (γ = 8.0 pS) (*B*, *D*, *F*) clamped to $V = -50$ mV. (*A*, *B*) Effective cable length, $e = d/\lambda$, as a function of mean agonist-induced current. (*C*, *D*) Ratio of variance to mean, *r*, as a function of mean agonist-induced current. (*E*, *F*) Ratio of variance to mean versus mean current plotted for different linear channel densities *n* (channels/μm).

conductance of the Ca^{2+}-activated olfactory channels) and γ = 8.0 pS (the value found for the cAMP-activated channels in our experiments). For Fig. 1 *A–D*, both channels are taken to have a linear density of 100 μm^{-1}. The ratio of conductance from ligand-gated channels to the basal conductance (*K* in Eq. 4) is 16 for the small channels and 160 for the large channels. Fig. 1 *A* shows *e* as a function of mean channel-induced current for the small channels. The cross-over point, $e = 1$, occurs at a current of 30 pA, about 44% of the maximum current (68 pA). The ratio of variance to mean for this case is shown in Fig. 1 *C*, and is seen to be pretty much linear. However, the observed line deviates considerably from that of a hypothetical space-clamped cilium having the same number of channels (3000). Thus the current intercept from which we infer the channel density occurs at 68 pA, whereas the same channels in a space-clamped preparation would yield a maximum current of 120 pA.

Fig. 1, *B* and *D*, shows exactly the same cable conditions and channel density, but for the large channels. The cable effects are now more pronounced. The cross-over point, $e = 1$, occurs at the same current as before, $\bar{I}$ = 30 pA, but this value of current is now only about 11% of the maximum current (265 pA). Similarly, the maximum current is now much smaller than the current for the hypothetical space-clamped channels (1200 pA). For the large channels, the ratio of variance to mean departs considerably from a linear plot, and for currents above 100 pA fits well to the infinite-cable parabola (Fig. 1 *D*).

Fig. 1, *E* and *F*, shows families of ratio versus mean plots for the two different channels plotted over the range of observed channel densities. Fig. 1 *E* shows the small channels at densities ranging from 32 to 100 per micron. The plots are always linear. Fig. 1 *F* shows the large channels at densities ranging from 14 to 100 per micron, illustrating how the plots change shape as channel density increases.

The analysis of this section explains how the cable-modified variance and mean expressions fitted to the cable noise data can be used to extract the conductances and densities of the channels.

RESULTS

Electrical recordings were made from single frog olfactory cilia. Each cilium was sealed inside a patch pipette and excised from the cell, so that the cytoplasmic face of its membrane was exposed to the bath (Kleene and Gesteland, 1991a). The patch pipette was held at a constant voltage while the cytoplasmic face of the cilium was exposed to different concentrations of agonists. We measured the mean current and the variance about the mean current and then used stationary noise analysis to estimate the channel characteristics. The cable-like structure of the cilium made it necessary to develop a cable-corrected noise analysis to interpret the mean current and the variance about the mean current in terms of the fluctuations in channel gating (see Methods/Theory). Basically, the cilium is not properly space clamped in this configuration, and hence the voltage is not constant along the length of the cilium, so that channels at different locations contribute differently to the current fluctuations at input. To test the validity of our theory, we first set out to measure the characteristics of the cAMP-activated channels with the cable-corrected noise analysis method. These estimates can be compared to channel characteristics that are known from studies of single-channel recordings of cAMP-activated channels.

Noise analysis of cAMP-activated channels in excised cilia

Excised cilia were held at −50 mV in symmetrical NaCl solutions. Recordings of the cAMP-activated channels were made in the absence of divalent cations, because these are known to reduce the channel conductance. This also eliminated a secondary Cl^- current that occurs in the presence of external Ca^{2+} (Kleene, 1993). The mean current and the variance were measured for cilia exposed to cAMP concentrations from 0.05 μM to 100 μM. The maximally activated currents vary greatly from cilium to cilium and do not correlate to the lengths of the cilia (Kleene et al., 1994). The maximum cAMP-activated current in this study ranged from 60 to 460 pA ($n = 6$). The ratio of maximum induced current to ciliary length ranged from 2.4 to 10.7 pA/μm ($n = 6$).

Two examples of the variance-versus-mean measurements are given in Fig. 2. The measurements in Fig. 2 *A* are for a cilium with a peak current density of 2.4 pA/μm, and those in Fig. 2 *B* are for a cilium with a higher peak current density, 7.8 pA/μm. The fitting of the data to the cable-corrected equations was made easier by replotting the data as variance/mean versus mean (Fig. 2, *C* and *D*).

For a space-clamped cilium, the plot of variance/mean versus mean current is a straight line that intersects the y axis at i (i = the single-channel current) for $p = 0$ (i.e., observed $\bar{I} = 0$) and the x axis at $\bar{I} = ndi$ (n = number of channels per unit length and d = length of cilium) for $p = 1$. For an infinite cable, the plot of variance/mean versus mean current is a parabola that intersects the y axis at $i/2$ for $p = 0$ ($\bar{I} = 0$), and the x axis at $(niV_0g_0\lambda_0^2)^{1/2}$ for $p = 1$ (V_0 = voltage at input, g_0 = basal membrane conductance, and λ_0 = basal space constant). The data for the cAMP-activated current showed features that were intermediate between these two extreme situations (Fig. 2, *C* and *D*).

We fit the data to the cable-corrected noise equations for the variance/mean ratio, $r(p)$, and the mean current, $\bar{I}(p)$, parameterized for the open probability, p (as given in Eqs. 4, 7, and 11):

$$r(p) = \gamma V_0(1 - p)\left[1/2 + \frac{d/\lambda(p)}{\sinh(2d/\lambda(p))}\right], \quad (15a)$$

$$\overline{I(p)} = np\gamma V_0\lambda(p)\tanh(d/\lambda(p)), \quad (15b)$$

$$\lambda(p) = \lambda_0[1 + (n\gamma p)/g_0]^{-1/2}. \quad (15c)$$

To use the cable-corrected noise equations, we have to know the basal cable properties of each cilium. The longitudinal resistance of the cilium, r_i, was estimated to be 11 MΩ/μm. The longitudinal resistance is related to the resistivity of the intracellular medium by

$$r_i = 4R_i/(\pi D^2), \quad (16)$$

where r_i = intracellular resistance to axial flow of current (per unit length), R_i = intracellular resistivity (assumed to be 70 Ω cm), and D = ciliary diameter (assumed to be 0.28 μm).

The length of the cilium, d, and the basal input impedance, G_{input}, were measured before and after each experiment. The basal input impedance has to be corrected for the shunt (i.e., the leak across the seal around the pipette tip), which could constitute a large part of the measured basal impedance. We were unable to measure the shunt in these experiments, but the shunts in standard solutions were previously estimated to average 175 pS ($n = 20$, range 97–330 pS; unpublished data from Kleene, 1992). Here we used 175 pS as the standard value to correct for the shunt. Then, with the estimated values of r_i, d, and G_{input}, we solved a transcendental equation in λ to find the basal membrane conductance g_0 (pS/μm) and the space constant λ_0 for each cilium (Kleene et al., 1994).

The cable-corrected noise equations, with the estimates of g_0, λ_0, and d for each cilium, were fitted by eye to the data. The fits give an estimate of the single-channel conductance, the density of channels, and the maximum open probability of the channels. The estimated single-channel conductance for the cAMP-activated channel was 8.3 pS ± 2.3 pS ($n = 6$). The channel density was 59 ± 38/μm length ($n = 6$, range 14–100). The maximum open probability was found to be 0.70 ± 0.095 ($n = 6$). In Fig. 2, *E* and *F*, we show how $e = d/\lambda(p)$ varies with mean current for these two cilia. The parameter e reaches 1 at a low agonist concentration for both cilia. A value of $e > 1$ means that only channels within approximately one length constant from the clamped end contribute to the observed macroscopic current. Thus as the agonist concentration is increased, one

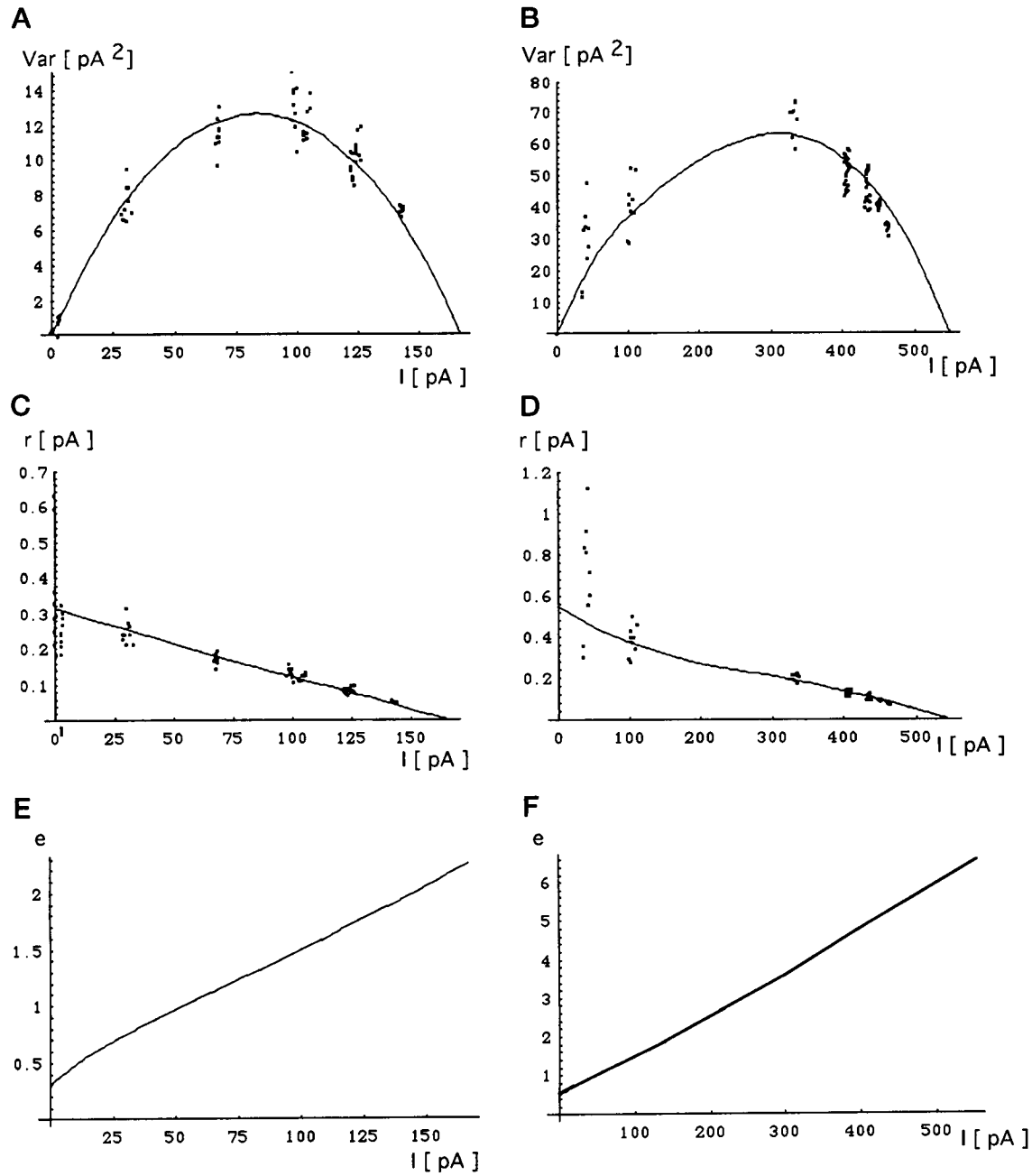

FIGURE 2 Variance analysis of cAMP-activated current. (*A*) Variance versus mean for a cAMP-activated current in a cilium of length 65 μm. In the absence of cAMP, the input conductance was 259 pS for this cilium. The shunt was assumed to be 175 pS. The estimated single-channel current is 0.33 pA. The number of channels is 18 channels/μm. (*B*) Variance versus mean for a cAMP-activated current in a cilium of length 60 μm. In the absence of cAMP, the input conductance was 540 pS for this cilium. The shunt was assumed to be 175 pS. The estimated single-channel current is 0.6 pA. The number of channels is 100 channels/μm. (*C*) Plot of variance/mean versus mean for the data in *A*, with the same fitted parameters as in *A*. (*D*) Plot of variance/mean versus mean for the data in *B*, with the same parameters as in *B*. (*E*) Effective cable length, $e = d/\lambda$, as a function of mean agonist-induced current for the data in *A*. (*F*) Effective cable length, $e = d/\lambda$, as a function of mean agonist-induced current for the data in *B*.

essentially records from a smaller and smaller membrane area, so that without the cable correction, one would greatly underestimate the channel density (see Fig. 1 *D*).

Noise analysis of the Ca^{2+}-activated current

A Ca^{2+}-activated Cl^- current has also been implicated in the olfactory response of the cilium. No channel properties are known for this component of current, because no single-channel recordings or noise analysis has been reported for this current. This is probably because the small size of this current makes it hard to analyze in small membrane patches. We can record from a whole excised cilium and, with our cable-corrected noise analysis, estimate the channel properties from the macroscopic current. Different calcium concentrations from 0.1 μM to 300 μM were applied to the

cytoplasmic surface of the cilium. With the cilium clamped at the input to −40 mV, the application of calcium induced a maximum current ranging from 31 pA to 61 pA (n = 6). As with the cAMP-activated current, there was no correlation between maximum current and ciliary length for the Ca^{2+}-activated current (Kleene et al., 1994). The maximum current density in a cilium ranged from 0.62 to 2.4 pA/μm (n = 6). The current densities of the Ca^{2+}-activated currents are smaller than the range seen for the cAMP-activated current. The Ca^{2+}-activated current is therefore recorded under conditions more closely approaching space clamp than the cAMP-activated current. Fig. 3, *A* and *B*, shows the

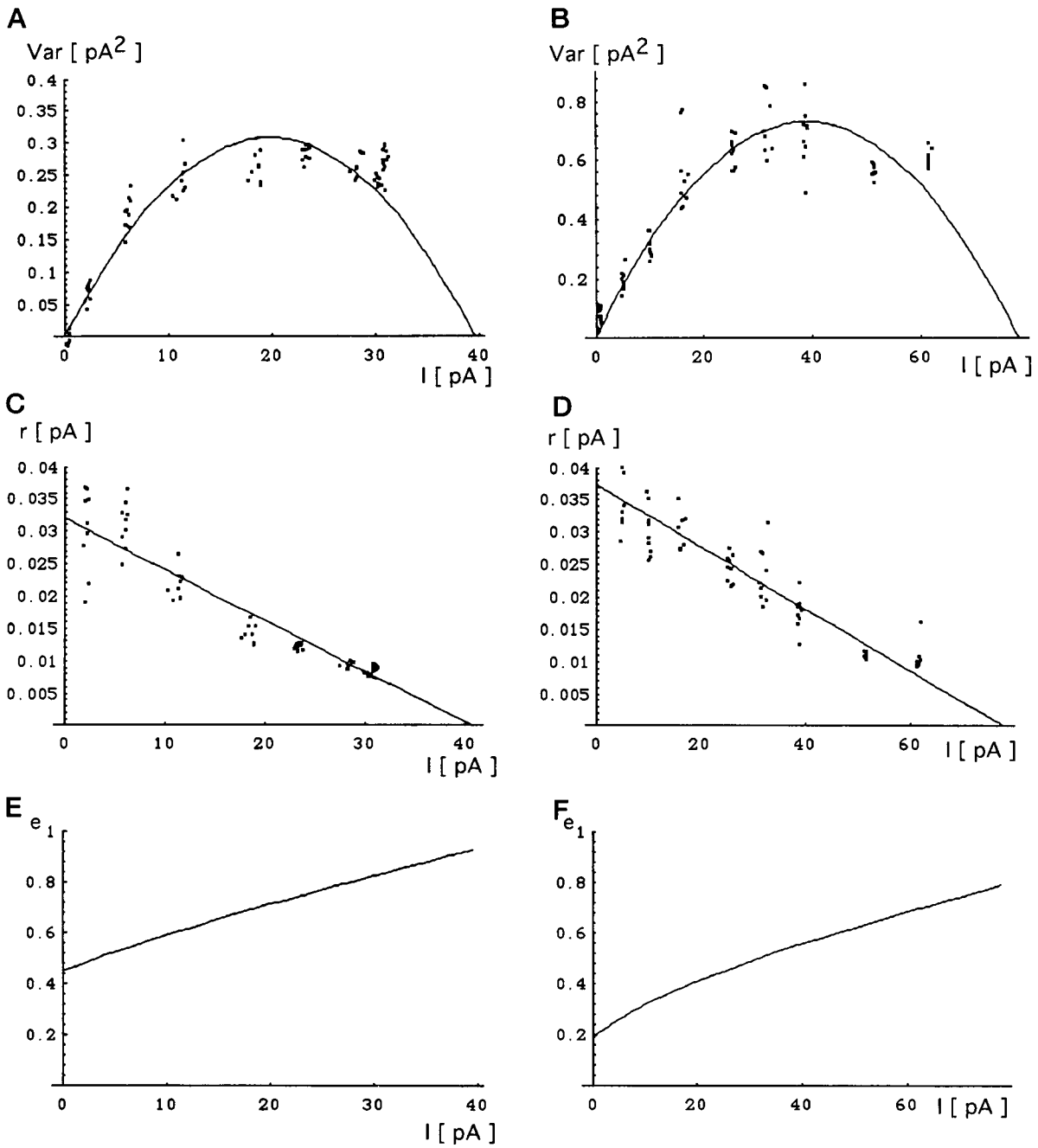

FIGURE 3 Variance analysis of Ca^{2+}-activated current. (*A*) Variance versus mean for a Ca^{2+}-activated current in a cilium of length 50 μm. In the absence of Ca^{2+}, the input conductance was 500 pS for this cilium. The shunt was assumed to be 175 pS. The estimated single-channel current is 0.032 pA. The number of channels is 29 channels/μm. (*B*) Variance versus mean for a Ca^{2+}-activated current in a cilium of length 25 μm. In the absence of Ca^{2+}, the input conductance was 230 pS for this cilium. The shunt was assumed to be 175 pS. The estimated single-channel current is 0.037 pA. The number of channels is 100 channels/μm. (*C*) Plot of variance/mean versus mean for the data in *A* with the same fitted parameters. (*D*) Plot of variance/mean versus mean for the data in *B* with the same parameters. (*E*) Effective cable length, $e = d/\lambda$, as a function of mean agonist-induced current for the data in *A*. (*F*) Effective cable length, $e = d/\lambda$, as a function of mean agonist-induced current for the data in *b*.

variance versus mean data for two cilia, with current/length ratios of 0.64 and 2.4 pA/μm. The plots of variance/mean versus mean current (Fig. 3, *C* and *D*) are more linear than the curves for the cAMP-activated current. This shows that the Ca^{2+}-activated current is more space-clamped, as expected from the lower maximum current/ciliary length ratio. We used the cable-corrected equations to fit the data, this time also with 175 pS as the value for the shunt.

The estimated single-channel conductance for the Ca^{2+}-activated channel is 0.8 $\pm$ 0.09 pS (n = 5). The channel density is 69 $\pm$ 30/μm length (n = 5, range 32–100). The maximum open probability was found to be 0.61 $\pm$ 0.04 (n = 5). In Fig. 3, *E* and *F*, we show how $e = d/\lambda(p)$ varies with mean current for these two cilia. The parameter e does not reach 1, even at saturating agonist concentrations for either cilium.

Power spectra of the cable currents

Fig. 4 *A* shows the power spectra for the cAMP-activated current. The difference spectra can be fitted with the sum of two Lorentzians when the background spectrum (0 cAMP) has been subtracted. The two time constants are 7.45 $\pm$ 0.78 ms and 0.165 $\pm$ 0.035 ms for 1 μM cAMP (n = 2).

The power spectra of the Ca^{2+}-activated current can be fitted to a sum of two Lorentzians when the background spectrum (0.1 μM free Ca^{2+}) has been subtracted (Fig. 4 *B*). The two time constants are 8.9 $\pm$ 0.29 ms and 0.52 $\pm$ 0.035 ms for 10 μM calcium (n = 2).

The fact that the spectra can be fitted with Lorentzians and are not modified by the "1/*f*" cable filter justifies the assumption that the DC treatment of the cable noise is adequate (see Theory). Both current components exhibit two-Lorentzian spectra over a range of agonist (i.e., cAMP, Ca^{2+}) concentration. In both cases, the corner frequency of the lower-frequency Lorentzian increases with increasing agonist dose while the higher frequency Lorentzian component remains invariant. Thus the lower frequency component probably represents events that are agonist-induced channel openings, and the high-frequency component shows the flickering of open channels.

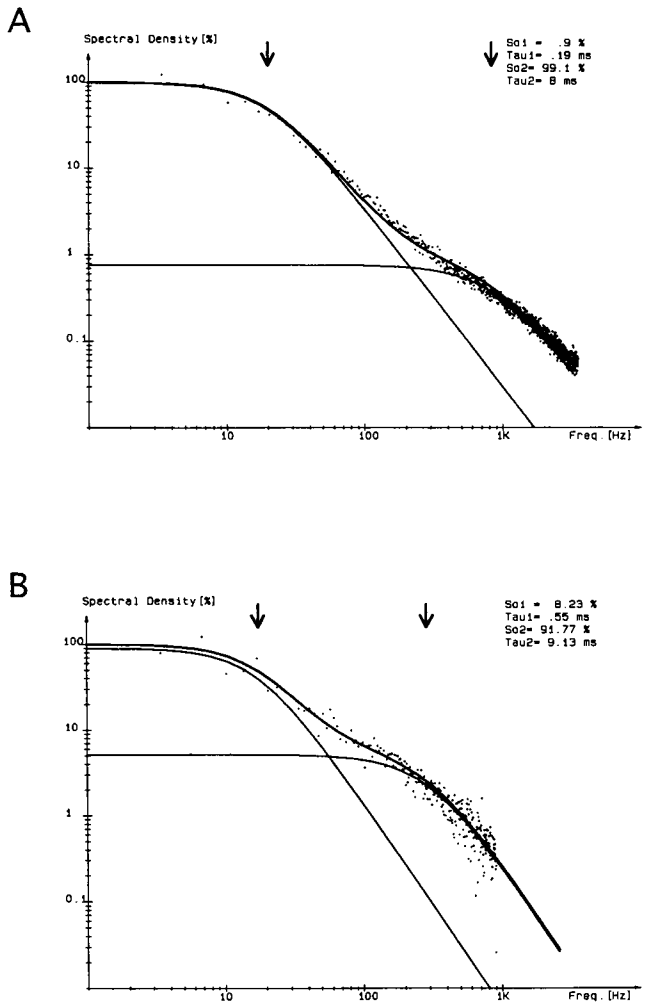

FIGURE 4 Power spectra for the cAMP-activated and Ca^{2+}-activated current. (*A*) Power spectrum for the cAMP-activated current for a cAMP concentration of 1 μM cAMP. A background spectrum recorded in the presence of 0 cAMP has been subtracted. The difference spectrum is fitted with two Lorentzian spectra. The time constants for this cilium are 8.0 ms and 0.19 ms for 1 μM cAMP. The cilium was held at -50 mV. (*B*) Power spectra for the Ca^{2+}-activated current for a concentration of 10 μM Ca^{2+}. A background spectrum recorded in the presence of 0.1 μM Ca^{2+} has been subtracted. The difference spectrum is fitted with two Lorentzian spectra. The time constants for this cilium are 9.13 ms and 0.55 ms. The cilium was held at -30 mV.

DISCUSSION

By analyzing the noise at the input of the ciliary cables we have been able to characterize the single-channel parameters for two different agonist-activated channels that contribute to the olfactory response at the cilium.

The channels activated by internal cAMP have a unitary conductance of 8.3 $\pm$ 2.3 pS in the absence of divalent ions. The power spectrum for this channel can be fitted with a two-Lorentzian spectrum. The noise experiments additionally yield the channel density, which is quite variable from cilium to cilium but averages approximately 59 $\pm$ 38 channels/μm or, on average, 67 channels/μm^2 (using 0.28 μm as the ciliary diameter; Kleene et al., 1994).

In the absence of cAMP, we find a channel activated by internal perfusion of Ca^{2+} that shows a unitary conductance of 0.8 $\pm$ 0.09 pS, too small to be observable by single-channel methods. The power spectrum for this channel can also be fitted with a two-Lorentzian spectrum. The channels conduct Cl^- ions (Kleene and Gesteland, 1991b) and have a linear density of approximately 69 $\pm$ 30 channels/μm or, on average, 78 channels/μm^2.

In interpreting the noise measurements, we have assumed that the ion channels are distributed uniformly throughout the ciliary membrane, because the variance and mean are calculated by integrating over uniform cylindrical slices of channel-containing membrane. Results from ciliary mem-

brane patches and intact receptor neurons both suggest that the cAMP-gated channels are distributed uniformly along the length of the cilium (Lowe and Gold, 1991; Kurahashi and Kaneko, 1993). We have also assumed that the ligand concentration is constant throughout the cilium. The steady-state ligand concentration in a cable decays with a length constant $\lambda = (Da/2P)^{1/2}$ (a = cable radius, D = diffusion constant in solution, P = membrane permeability for the ligand). We estimate that this length constant is at least an order of magnitude longer than the ciliary cables, and therefore we consider the ligand concentration as constant along the length of the cilium.

The results for the unit conductance of the cAMP-gated cationic channels in the ciliary cables constitute a check of the validity of the method, because the unit conductances of many such channels have been observed directly. Our values are comparable to those found for the cAMP-gated channel measured with other techniques. The conductances (summarized in Frings et al., 1992) range from 12 to 19 pS in the frog, but reach 55 pS in other vertebrates. Using the cable-corrected variance-to-mean analysis, our estimate of the unit conductance (8.3 pS) in the frog is slightly smaller than the unit conductances measured in single-channel patch-clamp experiments.

Fluctuation analysis of toad olfactory receptor neurons also gave a smaller estimate of the conductance for the cAMP-activated current than that observed by single-channel recording (Kurahashi and Kaneko, 1993). Small excised membrane patches were used in that study, so no cable correction was necessary. Still, the unit conductance inferred from the variance-to-mean plot (figure 3 of Kurahashi and Kaneko, 1993) appeared to be about 40% smaller than the conductance directly measured from single channels. The discrepancy may come about because of different ionic compositions or because of filtering of some flickering component of the channel noise. One possibility is suggested by the observation that expressed olfactory cAMP-gated channels show three substates at roughly equal conductance intervals (Root and MacKinnon, 1994). If the channel has substates, then it is likely that fluctuation analysis reveals the substate conductance and is therefore less than the single-channel conductance measured directly.

The similar estimates for the single-channel conductance obtained with our method and with excised patches, for the cAMP-activated channels, give us confidence in the accuracy of our cable-corrected noise analysis method. The two channel types studied were present at similar densities. Our estimate of the single-channel conductance of the Ca^{2+}-activated Cl^- channel is 10-fold smaller than the conductance of the cAMP-activated channel. The latter was measured in the absence of divalent cations. However, under physiological conditions, Ca^{2+} in the mucus reduces the unit conductance of the cAMP-gated channels to roughly 1.5 pS (Zufall and Firestein, 1993). In addition, Ca^{2+} appears to stabilize the closed state of the channel (Zufall et al., 1991b) and likely reduces its maximum open probability. These two effects of Ca^{2+} could explain the observation that the secondary Cl^- current accounts for up to 85% of the odorant-induced current (Lowe and Gold, 1993).

For both channel species, the densities of channels were not correlated with the length of the cilia. An earlier study found that the maximum inducible current was not correlated with ciliary length, but that the amplitudes of the cAMP-activated and Ca^{2+}-activated currents were correlated across the population of cilia (Kleene et al., 1994). There also seem to be large variations in channel densities between cilia (220-fold range for the cAMP-channels; Kleene et al., 1994). Our estimate of 67 channels/μm^2 for the cAMP-activated channels is in the range of densities reported in an earlier paper (average 205 channels/μm^2 with a 220-fold range; Kleene et al., 1994). Higher estimates of channel densities came from experiments done on excised patches from cilia (450–7000 channels/μm^2, Nakamura and Gold, 1988; 1750 channels/μm^2, Kurahashi and Kaneko, 1993). A possible explanation of the discrepancy between the patch recordings and the whole-cilium recordings could be that the patch observations tend to underestimate the true size of the membrane patch, which may be large and omega-shaped. This would lead to an overestimate of the channel density.

Errors in the cable analysis method

The analysis of the noise data depends on knowledge of the cable parameters of the cilium. These parameters include the length, diameter, core resistivity, and specific membrane resistance of the resting cilium. The lengths of individual cilia were accurately determined by inspection. The frog olfactory cilium has a diameter of 0.28 μm for the proximal part, but tapers to 0.19 μm in the distal portion (Menco, 1980). We assumed the cilium to be a cylinder of the proximal diameter, with a core resistivity of 70 Ω cm. Errors in the estimation of the diameter and resistivity of the ciliary core will give errors in the estimates of the density of channels. Assuming a diameter of the cilium of 0.24 μm, the average of proximal and distal diameters, would increase the channel density by up to 59% (Kleene et al., 1994). Within the limits of these uncertainties, our analysis still suggests that there is considerable real variation in channel density from cilium to cilium.

The basal specific membrane resistance and the basal length constants are obtained from measurements of the basal input conductance, which must be corrected by the unknown shunt conductance through the seal between the pipette and the cilium. Unpublished results from a previous study (Kleene, 1992) indicate that on average only about 35% of the basal input conductance is from the membrane. Thus there is considerable room for error in the determination of the basal cable properties. In the case of the cAMP-activated channels, this does not alter the estimates of the single-channel conductance or the channel density, because the channel-induced conductance becomes bigger than the basal conductance at rather low agonist concentration. In Fig. 5 we show the fit of the variance/mean versus mean

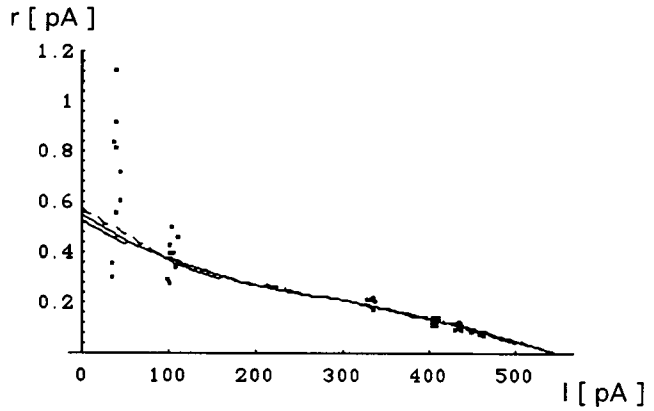

FIGURE 5 Fit of variance-to-mean ratio for three different values of basal shunt conductance. Plot of variance/mean versus mean for a cAMP-activated current in a cilium of length 60 μm. In the absence of cAMP, the input conductance was 540 pS for this cilium. The shunt was assumed to be 0 pS (*long dashes*), 175 pS (*solid line*), or 325 pS (*short dashes*). The estimated single-channel current is 0.6 pA. The number of channels is 100 channels/μm.

plot for a cilium with three diffferent estimated values for the shunt (0, 175, and 350 pS). The curves for these three cases differ only slightly from each other and give essentially the same estimates for channel density and single-channel conductance.

For the smaller Ca^{2+}-activated channels, different estimates of the shunt give a small variation in the estimated single-channel conductance. The uncertainty in the value of the shunt gives rise to an uncertainty in the value of the basal length constant, λ_0. When fitting data to the plots of variance/mean versus mean, alternative fits cannot differ by more than a factor of 2 for the unitary current, because the difference between the short cable ($d/\lambda_0 \ll 1$) and the infinite cable ($d/\lambda_0 \gg 1$) limits differ by only that much. This can be seen from the Theory section, in which it is shown that in the limit of an infinite cable the zero-current intercept is $i/2$ compared to i for the space-clamped case (Fig. 1 *D*). In general, the zero-current intercept is given by (from Eq. 11)

$$r \to i\left[\frac{2e_0 + \sinh(2e_0)}{2\sinh(2e_0)}\right], \quad \text{when } p \to 0. \qquad (17)$$

This gives $r = i$ for the space-clamped case (i.e., $e_0 \to 0$), and $r = i/2$ for the infinite cable case (i.e., $e_0 \to \infty$). For the Ca^{2+}-activated Cl^- current, e_0 was found to be 0.6 at most, which could introduce at most an error of ~10% into the estimate of the single-channel conductance. Thus cable noise can be considered to give a reliable lower limit to the channel conductance independent of uncertainties in the analysis.

This work was supported by a post-doctoral fellowship from the Wenner-Gren Center to HPL, by research grant 5-RO1-DC00926 from the National Institute on Deafness and other communication dissorders (National Institutes of Health) to SJK, and by NSF grant 8904462 to HL.

REFERENCES

DeFelice, L. 1981. Introduction to Membrane Noise. Plenum Press, New York.

Firestein, S., G. M. Shepherd, and F. Werblin. 1990. Time course of the membrane current underlying sensory transduction in salamander olfactory receptor neurones. *J. Physiol. (Lond.).* 430:135–158.

Frings, S., J. W. Lynch, and B. Lindemann. 1992. Properties of cyclic nucleotide-gated channels mediating olfactory transduction. *J. Gen. Physiol.* 100:45–67.

Frings, S., R. Seifert, M. Godde, and U. B. Kaupp. 1995. Profoundly different calcium permeation and blockage determine the specific function of distinct cyclic nucleotide-gated channels. *Neuron.* 15:169–179.

Jack, J. J., D. Noble, and R. W. Tsien. 1975. Electrical Current Flow in Excitable Cells. Clarendon Press, Oxford.

Kleene, S. J. 1992. Basal conductance of frog olfactory cilia. *Pflugers Arch.* 421:374–380.

Kleene, S. J. 1993. Origin of the chloride current in olfactory transduction. *Neuron.* 11:123–132.

Kleene, S. J. 1995. Patch-clamping of whole olfactory cilia. *In* Experimental Cell Biology of Taste, and Olfaction/Current Techniques, and Protocols. A. I. Spielman and J. G. Brand, editors. CRC Press, Boca Raton, FL. 347–352.

Kleene, S. J. 1996. Amplification properties of amphibian olfactory receptor currents. *Chem. Senses.* (in press).

Kleene, S. J., and H. C. Cejtin. 1994. Solving buffering problems with Mathematica software. *Anal. Biochem.* 222:310–314.

Kleene, S. J., and R. C. Gesteland. 1991a. Transmembrane currents in frog olfactory cilia. *J. Membr. Biol.* 120:75–81.

Kleene, S. J., and R. C. Gesteland. 1991b. Calcium-activated chloride conductance in frog olfactory cilia. *J. Neurosci.* 11:3624–3629.

Kleene, S. J., R. C. Gesteland, and S. H. Bryant. 1994. An electrophysiological survey of frog olfactory cilia. *J. Exp. Biol.* 195:307–328.

Kleene, S. J., and R. Y. K. Pun. 1996. Persistence of the olfactory receptor current in a wide variety of extracellular enviroments. *J. Neurophysiol.* 75:1386–1391.

Kurahashi, T. 1989. Activation by odorants of cation-selective conductance in the olfactory receptor cell isolated from the newt. *J. Physiol. (Lond.).* 419:177–192.

Kurahashi, T., and A. Kaneko. 1993. Gating properties of the cAMP-gated channel in toad olfactory receptor cells. *J. Physiol. (Lond.).* 466: 287–302.

Kurahashi, T., and T. Shibuya. 1990. Ca^{2+}-dependent adaptive properties in the solitary olfactory receptor cell of the newt. *Brain Res.* 515: 261–268.

Kurahashi, T., and K.-W. Yau. 1993. Co-existence of cationic and chloride components in odorant-induced current of vertebrate olfactory receptor cells. *Nature.* 363:71–74.

Kurahashi, T., and K.-W. Yau. 1994. Tale of an unusual chloride current. *Curr. Biol.* 4:256–258.

Lecar, H., and F. Sachs. 1981. Membrane noise analysis. *In* Excitable Cells in Tissue Culture. P. G. Nelson and M. Lieberman, editors. Plenum Press, New York. 137–172.

Lowe, G., and G. H. Gold. 1991. The spatial distributions of odorant sensitivity and odorant-induced currents in salamander olfactory receptor cells. *J. Physiol. (Lond.).* 442:147–168.

Lowe, G., and G. H. Gold. 1993. Nonlinear amplification by calcium-dependent chloride channels in olfactory receptor cells. *Nature.* 366: 283–286.

Menco, B. Ph. M. 1980. Qualitative and quantitative freeze-fracture studies on olfactory and nasal respiratory structures in frog, ox, rat, and dog. I. A general survey. *Cell Tiss. Res.* 207:183–209.

Nakamura, T., and G. H. Gold. 1987. A cyclic nucleotide-gated conductance in olfactory receptor cilia. *Nature.* 325:442–444.

Nakamura, T., and G. H. Gold. 1988. Single-channel properties of the ciliary cyclic nucleotide-gated conductance. *Chem. Senses.* 13:723–724.

Restrepo, D., J. H. Teeter, and D. Schild. 1996. Second messenger signaling in olfactory transduction. *J. Neurobiol.* 30:37–48.

Root, M. J., and R. MacKinnon. 1994. Two identical noninteracting sites in an ion channel revealed by proton transfer. *Science.* 265:1852–1856.

Zhainazarov, A. B., and B. W. Ache. 1995. Odor-induced currents in *Xenopus* olfactory receptor cells measured with perforated-patch recording. *J. Neurophysiol.* 74:479–483.

Zufall, F., and S. Firestein. 1993. Divalent cations block the cyclic nucleotide-gated channel of olfactory receptor neurons. *J. Neurophysiol.* 69:1758–1768.

Zufall, F., S. Firestein, and G. M. Shepherd. 1991a. Analysis of single cyclic nucleotide-gated channels in olfactory receptor cells. *J. Neurosci.* 11:3573–3580.

Zufall, F., S. Firestein, and G. M. Shepherd. 1994. Cyclic nucleotide-gated ion channels and sensory transduction in olfactory receptor neurons. *Annu. Rev. Biophys. Biomol. Struct.* 23:577–607.

Zufall, F., G. M. Shepherd, and S. Firestein. 1991b. Inhibition of the olfactory cyclic nucleotide-gated ion channel by intracellular calcium. *Proc. R. Soc. Lond.* B246:225–230.